Interannual Variations of Tropical Upper Tropospheric Divergence and Pacific Teleconnections during Northern Winter

C.-P. CHANG, M. S. PENG

Department of Meteorology
Naval Postgraduate School, Monterey, CA 93943, U.S.A.

AND

J. S. BOYLE

Naval Oceanographic and Atmospheric Research Laboratory
Atmospheric Directorate, Monterey, CA 93943, U.S.A.

ABSTRACT

A 15-year (1974-1988) data set based on the US Navy's tropical global band analysis is used to study the interannual variations of 200 mb winter flow over the Pacific. The divergence fields are free from numerical model prediction influences that typically exist in operational data sets, and agree well with the mean outgoing longwave radiation data. An out-of-phase variation between two major equatorial centers of large-scale divergence anomalies, one over the central Pacific and the other over the western extreme of the western Pacific (maritime continent), is most noticeable. A third major center of divergence anomalies is located southwest of the Mexican coast. This center also shows an out-of-phase variation with that in the equatorial central Pacific. Composite and single-point correlation studies support the notion that the teleconnection patterns are related to equatorial divergence anomalies. In particular, divergence forcing from the central Pacific appears important for the PNA pattern, and forcing from the maritime continent area appears important for a northeastward wave train pattern in the North Pacific. These two teleconnection patterns have streamfunction anomalies of the opposite sign over the northeastern Pacific. By examining the change of correlation patterns as the divergence base point is moved around the equatorial belt, the insensitivity of the teleconnection pattern with respect to tropical forcing locations as reported by several general circulation model simulations is observed only within limited regions. In the equatorial Pacific, the PNA correlation pattern changes slowly when the equatorial divergence base point is within 150^oE-120^oW. The pattern changes rapidly when the base point is moved outside of this region.

1. INTRODUCTION

The possible roles of tropical sea-surface temperature (SST) anomalies on the interannual variability of extratropical circulations have been the subject of many observational and modeling studies. The most prominent possible relationship is that between the tropical Pacific SST anomaly and the Pacific-North America (PNA) teleconnection pattern (Horel and Wallace, 1981). There are several interesting points that emerge from these studies. One of these results from general circulation model (GCM) simulations (e.g., Geisler *et al.*,1985; Blackmon *et al.*, 1987), and suggests that the response to forcing from the equatorial eastern Pacific SST is relatively insensitive to the longitudes of the SST anomalies. One possible explanation for this is that extratropical variability is more responsive to midlatitude SST anomalies than tropical anomalies, as suggested by the observational study by Wallace and Jiang (1987). However Pitcher *et al.* (1988), in a GCM study of the effect of SST anomalies in the North Pacific, found that during warm episodes the model response is approximately the sum of the forcing from midlatitude and tropical anomalies. Thus it is difficult to ignore the issues raised by the previous GCM results concerning the effects of tropical SST anomalies.

A number of theoretical and modeling studies have been carried out to explain the insensitivity of the extratropical response to tropical SST anomaly longitude. Since theories with a zonally symmetric basic state automatically give an extratropical response that depends on the longitude of the tropical forcing, the two-dimensional horizontal variation of the time-mean flow was incorporated in these studies. The results of these studies led to several alternative theories that proposed to explain the insensitivity problem. The proposed theories include ones based on Rossby wave generation due to significant interaction between divergent flow and strong westerly meridional shear, whose location is quasi-fixed by the East Asian subtropical jet (e.g., Sardeshmukh and Hoskins, 1988); the preferred response distribution due to barotropic instability of the time-mean flow (Simmons *et al.*, 1983); and wave energy channeling guided by the sign of the time-mean zonal flow (Webster and Chang, 1988). The first two are entirely different mechanisms but which may coexist, while the first and the last are more mutually exclusive.

Another interesting question concerns the possible relationship between forcing from the western extreme of the equatorial western Pacific (the "maritime continent" area) and the teleconnection patterns in the North Pacific (Livezey and Mo, 1987). Simmons *et al.* (1983), Geisler *et al.* (1985), Branstator (1985) and Blackmon *et al.* (1987), in linear and GCM studies, have considered the possibility that anomalous heating in the maritime continent area may also give rise to the northern cell (over the northeastern Pacific) of the opposite PNA

pattern. It has long been reported that there are often opposite fluctuations in precipitation between the equatorial western Pacific and the equatorial central Pacific, and that out-of-phase oscillations in the divergence and outgoing longwave radiation (OLR) fields exist in time scales from intraseasonal to interannual (e.g., Lau and Chang, 1987; Livezey and Mo, 1987.) Thus anomalous heating in the equatorial western Pacific-maritime continent area normally occurs during cool central Pacific SST periods. This complicates the analysis of the different roles of anomalous heating in the two regions. Furthermore, in GCM studies the evidence of the maritime continent effects is less conclusive than that of the SST anomalies in the tropical central Pacific. For example, in studying the effects of mountains in a GCM, Blackmon *et al.* (1987) produced cases with a positive precipitation anomaly over Indonesia, without a negative PNA over the North Pacific. Also, Pitcher *et al.* (1988) did not produce a negative PNA pattern during cool central Pacific SST anomalies. It is not known whether these two results are due to the same or different causes. A question may also be raised as to whether a negative PNA that is correlated with tropical heating anomalies is independently identifiable, rather than simply reflecting a residual when very strong PNA signals are removed from the long-term mean.

The forcing of extratropical response by tropical SST or tropospheric heating anomalies involves complex dynamical and thermodynamic processes throughout the troposphere. For example, vertical wind shear or other baroclinic effects may be important for tropical cumulus heating to force an extended meridional propagation (Chang and Lim, 1983; Lim and Chang, 1986; Kasahara and Silva Dias, 1986). However, at approximately equivalent barotropic levels, the barotropic vorticity equation should describe reasonably well the forcing-response dynamics, and 200 mb is close to being equivalent barotropic (Sardeshmukh and Hoskins, 1988). Thus an analysis of the divergence and vorticity data at 200 mb may provide clues to the relationship between tropical SST and heating anomalies and the teleconnection patterns. However, such an analysis is rarely done and most studies on the effect of tropical heating are either based on OLR data, or on GCM simulations with prescribed SST anomalies. It may be noted that while large-scale OLR and divergence over the tropics are positively correlated, significant differences exist between the two. For example, Weickmann and Khalsa (1990) showed that for the 30-60 day period band the equatorial 150 mb velocity potential and the OLR patterns propagate at speed differ by a factor of 2 to 3.

There are several reasons why tropical divergence analyses, most of which are produced by four-dimensional data assimilation cycles in operational numerical weather prediction (NWP) systems, are normally not suitable for teleconnection studies. First, the NWP divergence field is often overwhelmed by model forecast divergence, and as a result the divergence is often significantly underestimated

(Lambert, 1989; Unden, 1989). Another problem is that the interannual time scale of the teleconnections requires the use of a relatively long period of data, but the NWP systems are changed frequently. Therefore NWP analyses data in the tropical region usually have different characteristics from one year to another, with the most significant inhomogeneous problem occurring in the tropical divergence (Trenberth and Olson, 1988).

In this study, a 15-year (1974-1988) data set of the US Navy's operational tropical global band analysis is used to study the possible relationships between tropical Pacific divergence and the teleconnection patterns at 200 mb during northern winter. (The data set contains 14 complete winters, each from December to the next February). In particular, we will focus on the relative roles of the divergence over the tropical central Pacific and the maritime continent in the development of the PNA and negative PNA patterns, and the sensitivity of the extratropical responses to forcing location. The analysis uses 6-hour persistence as the first guess, therefore its divergence field is not influenced by numerical predictions as is the case in most of the present data sets produced by global NWP systems. The analysis scheme also remained unchanged for the entire 15 years. Thus we have a relatively long-term homogeneous data set to study the interannual variations.

2. DATA SOURCE AND ANALYSES

a. Global band analysis

The wind data used are the operational analyses of the Global Band Analyses (GBA) of the Fleet Numerical Oceanographic Center (FNOC) during 1974-1988. These data were produced four times daily by objective procedures on a Mercator grid which extends from 60°N to 40°S. The use of the Mercator secant projection resulted in a change in the distance between grid points from 140 km at 60°N to a maximum value of 280 km at the equator. The objective analysis scheme was designed to take advantage of all the reports in the operational data base: surface synoptic, aircraft, pilot balloons, rawindsonde and satellite data.

The analysis was performed every six hours for the surface, 700, 400, 250 and 200 mb levels, using a successive corrections method, with the six-hour persistence used as the first guess. Both wind and temperature were analyzed and then adjusted by a set of numerical variational analysis (NVA) equations which incorporated the dynamical constraints of the momentum equations with friction included in the surface layer (Lewis and Grayson, 1972). Temperature and wind fields were adjusted subject to mutual constraints on the fields. However, the 200 mb wind data used here served only as a boundary condition for NVA and were not subject to the adjustment.

b. Computation of streamfunction and velocity potential

To represent the large-scale rotational and divergent motions, the streamfunction (ψ) and velocity potential (χ) were computed, respectively, from the following equations:

$$\nabla^2 \psi = \zeta, \tag{1}$$

$$\nabla^2 \chi = -D, \tag{2}$$

where relative vorticity is

$$\zeta = \frac{\partial v}{\partial x} - \frac{\partial u}{\partial y},$$

and divergence is

$$D = \frac{\partial u}{\partial x} + \frac{\partial v}{\partial y}.$$

Both ζ and D were computed using centered differences on the GBA Mercator grid.

Eq. (2) was solved using the boundary condition that $\chi = 0$ at the north and south boundaries, which are at 60°N and 40°S, respectively. The method used to compute ψ was essentially method II of Shukla and Saha (1974). This technique uses the previously computed values of χ to formulate boundary conditions for ψ. Comparison with the global fields produced by the National Meteorological Center (NMC) for the years since the NMC global product has become available indicates that the solutions are not sensitive to the boundary condition between 50°N and 30°S for all the months used in this study. Extensive comparisons between χ and divergence fields also confirm that while the former is inversed Laplacian of the latter, it represents very well the smoothed pattern of divergence, both for time means and anomalies.

The use of persistence as the first guess, rather than using short-term NWP predictions, may cause a concern for data-sparse tropical area. However, comparison between the monthly-mean 200 mb divergence from GBA and the OLR data (Boyle and Chang, 1984, and Lau and Boyle, 1987) shows that the agreement is at least as good as that between the four-dimensional assimilated NWP analysis and OLR. In addition, daily GBA divergence data in the tropical Pacific have been used successfully in studying synoptic time scale variations (e.g., Chang and Lum, 1985; Lau and Chang, 1987). Furthermore, the Australian Bureau of Meteorology also uses persistence as the first guess in its tropical regional analysis over the western Pacific since September 1983. By comparing with the ECMWF gridded data, Hendon (1988) concluded that the large-scale tropical circulation is depicted quite well in the Australian analysis.

3. TIME MEAN FIELDS

In this study, anomalies of the 200 mb streamfunction (ψ) and velocity potential (χ) for each of the three-month winter seasons, and each of the individual months within the season, are analyzed. These anomalies are calculated as departures from their respective 15-year means. In order to give an overall perspective of the 200 mb flow fields before the discussion of the anomalies, the 200 mb mean ψ and χ for the entire 15 winters are shown in Figs. 1a-b, respectively.
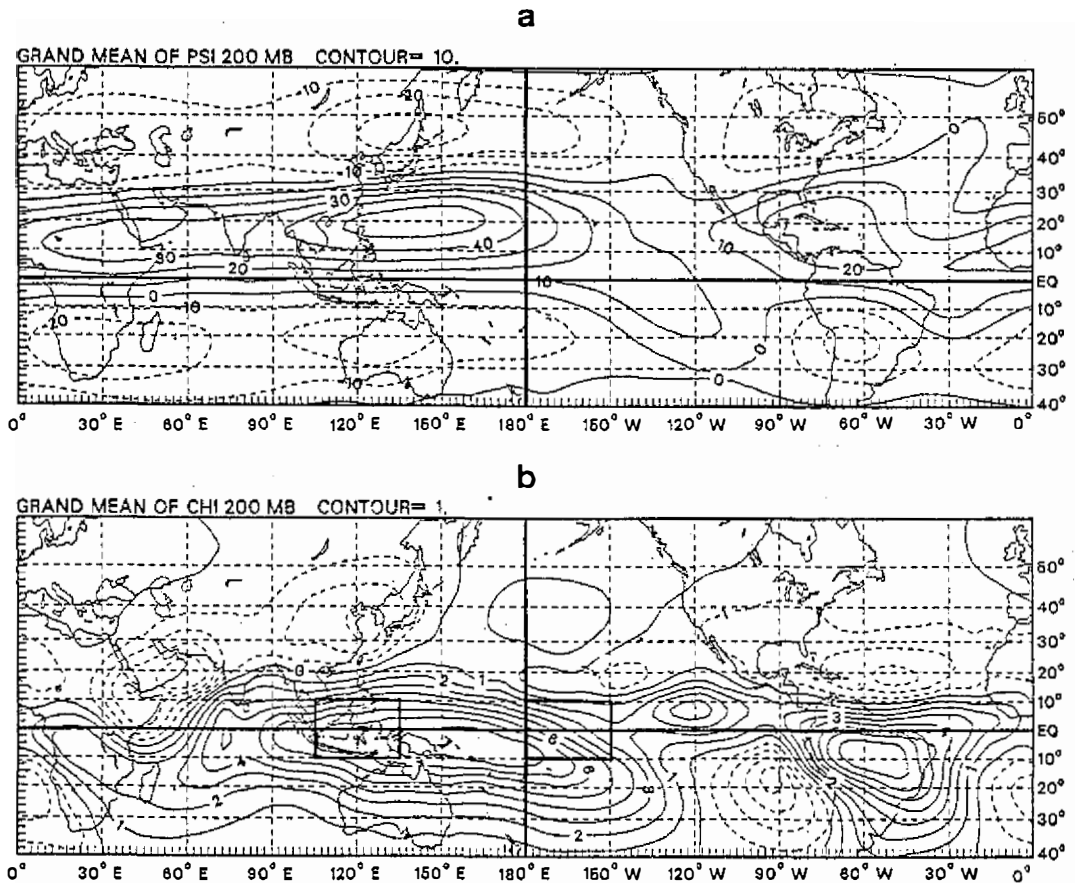
a

GRAND MEAN OF PSI 200 MB   CONTOUR= 10.

b

GRAND MEAN OF CHI 200 MB   CONTOUR= 1.

Fig. 1. 15-winter mean 200 mb (a) streamfunction (ψ), and (b) velocity potential (χ), both with units 106 $m^2\ s^{-1}$. Positive values indicated by solid lines and negative values by dashed lines. The central Pacific and maritime continent anomalous divergence centers are indicated by rectangulars in *Fig.* 1b.

The mean ψ field (Fig. 1a) in the northern hemisphere is dominated by the familiar patterns of two south-north anticyclone-cyclone pairs. The predominant one over East Asia- western Pacific encompasses a longitudinal domain of about one half of the globe, while the secondary one is more restricted over the

vicinity of North America. The strength of the mean East Asia subtropical jet is produced by the quasi-stationary location of the strong ψ gradients locally, while over North America the gradients are considerably weaker due to the migratory nature of the jet there. At the equator, the antisymmetric distribution in ψ correspondes to a symmetric height distribution with three anticyclonic cells in the southern hemisphere. The extent of each of these circulations are comparable to their northern subtropical counter-parts, but the strength of the one over the Australia-southwestern Pacific is much weaker than the one over East Asia-northwestern Pacific.

The mean χ field (Fig. 1b) shows an extensive equatorial divergence area over the same western Pacific longitudes as the ψ center shown in Fig. 1a. The area extends toward west-southwest in the central Pacific, which is a manifestation of the South Pacific Convergence Zone (SPCZ). Previous winter-mean 200 mb divergence calculated by Krishnamurti et al. (1973), Murakami and Unnunayar (1977) and Arkin et al. (1986) all showed a strong east-west (Walker-type) divergent component over the tropical Pacific that is at least comparable to the north-south (Hadley-type) component. However, Fig. 1b shows that the Hadley-type component is much more dominant. Compared to the previous studies the structure of the SPCZ is also better defined. Furthermore, Fig. 1b shows an outflow region in the equatorial eastern Pacific centered near 120°W that is totally absent from the NWP-based analyses by Murakami and Unnunayar (1977) and Arkin et al. (1986). It is interesting to note that this feature is present in Krishnamurti et al.'s (1973) subjective analysis of the January-March 1969 data, and is consistent with long-term OLR distribution where the OLR minimum in the entire tropical eastern Pacific is located. Other significant differences from the NWP-based studies include the locations of the divergence centers over South America and Africa. In Fig. 1b they are near 10°S rather than the equator as found in Murakami and Unnunayar (1977) and Arkin et al. (1986). Again, the present distribution agrees much better with the OLR observations.

4. COMPOSITE OF ANOMALIES

The seasonal (December-February) averaged data are used to compute the streamfunction and velocity potential anomalies from their long-term means. Inspection of each year's χ field (not shown) can readily identify two major centers of χ anomalies, one over the equatorial central Pacific (CP) and the other over the equatorial western Pacific near the maritime continent (MC). As expected, they are often of opposite signs. However, within their respective general areas the location of both centers varies considerably from year to year. It is interesting that neither anomaly center is located in the center of the

long-term mean at about 5°S, 165°E (see Fig. 1b).

The anomalies are composited in two different ways. The first is according to the central Pacific SST anomalies. This is done by inspecting the time series of a standardized equatorial SST anomaly near 170°W plotted by Kousky and Leetmaa (1989). Fig. 2 shows this plot which was based on the equatorial portion of a ship track that runs between Fiji and Hawaii. Based on this time series, four winters of warm SST anomalies ("El Nino") and four winters of cool SST anomalies ("Anti-El Nino") are selected for compositing. Table 1 lists the winters selected.

Table 1. Winters selected for El Nino, Anti-El Nino, and positive maritime continent (MC) divergence composites

El Nino: 1977-78, 1982-83, 1986-87, 1987-88

Anti-El Nino: 1974-75, 1975-76, 1983-84, 1984-85

Maritime continent: 1974-75, 1976-77, 1980-81, 1981-82, 1983-84, 1984-85, 1985-86

The El Nino composites (Fig. 3) show the expected PNA teleconnection pattern in the ψ field and the positive divergence anomaly over central Pacific (CP) in the χ field. It is well known that the 1982-83 season was a very strong El Nino case, and Fig. 3 may be dominated by this single period. However, the three other El Nino winters (not shown) all show the same general patterns of ψ and χ anomalies. The Anti-El Nino composites (Fig. 4) have strong negative correlations with the El Nino composites, and the streamfunction anomaly shows a clear signal of a negative PNA teleconnection pattern. In order to ascertain that the negative PNA pattern is not simply a reflection of the difference between the long-term mean and the strong PNA signal, the six winters that do not belong to either El Nino or Anti-El Nino are also composited and the results are shown in Fig. 5. It is clear that these in-between years do not show any organized patterns that are similar to the PNA or negative PNA patterns in either the ψ or the χ anomalies.

There are other features in the El Nino composites that are noteworthy. In Fig. 3a marked antisymmetric distributions of the anomalous ψ centers (symmetric in height) about the equator can be found in three places. The most prominent antisymmetric couplet is in the (maritime continent) MC longitudes
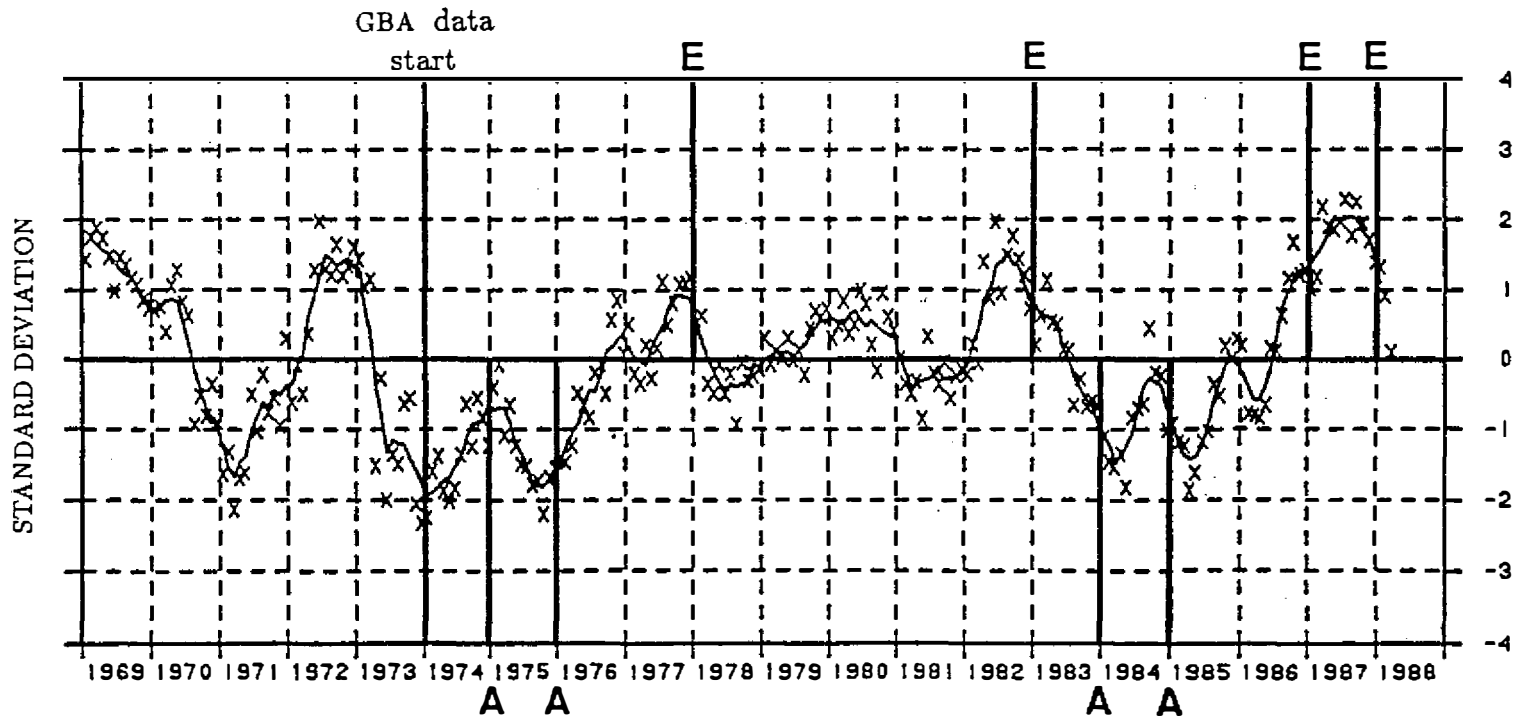
Fig. 2. Time series of a standardized equatorial SST anomaly near 170°W based on the equatorial portion of a ship track that runs between Fiji and Hawaii (adapted from Kousky and Leetmaa, 1989). The selected El Nino and Anti-El Nino years are labeled by E and A, respectively.
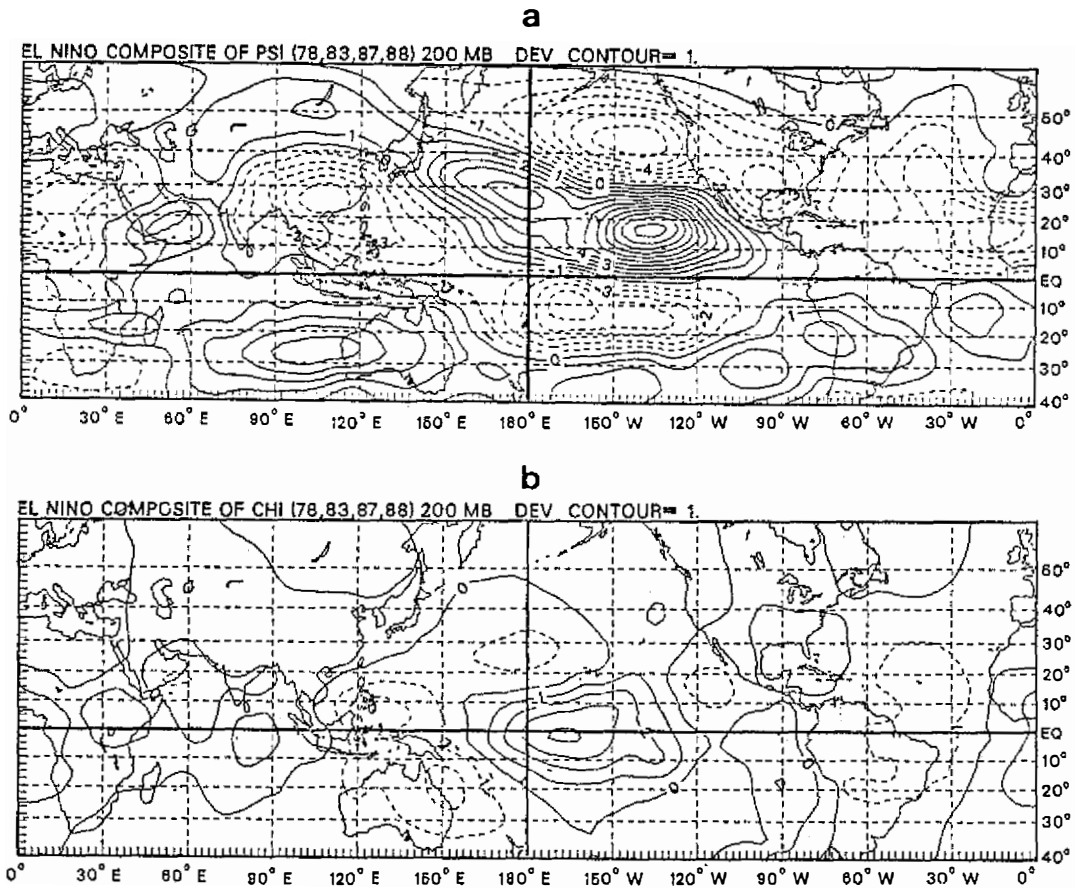
a

EL NINO COMPOSITE OF PSI (78,83,87,88) 200 MB   DEV CONTOUR= 1.

b

EL NINO COMPOSITE OF CHI (78,83,87,88) 200 MB   DEV CONTOUR= 1.

Fig. 3. Composites of the anomalies of the four El Nino winters. (a) ψ, and (b) χ. The counter interval for ψ is 10^7 m^2 s^{-1}, for ψ is 10^6 m^2 s^{-1}.

centered between 90°E-120°E, with both the northern and southern centers located about 25-30° from the equator. The other two are in the central Pacific and the eastern Atlantic, respectively, although the centers in the former are mis-aligned by about 30° of longitude. The centers of these two pairs are also more equatorward, within 20° from the equator. Fig. 3b shows that the three couplets are in the vicinity of the anomalous equatorial divergence regions in Indonesia, central Pacific and Atlantic, respectively. The signs of the ψ anomalies relative to those of the χ anomalies are consistent with the Rossby response to heating in linear equatorial wave theory (Gill, 1980, Chang and Lim, 1983), although the longitudinal position of the northern anticyclinic center relative to the divergence center is shifted from the theoretical northwest position to the observed north position.

The anomalous χ field in the El Nino composites (Fig. 3b) shows that the
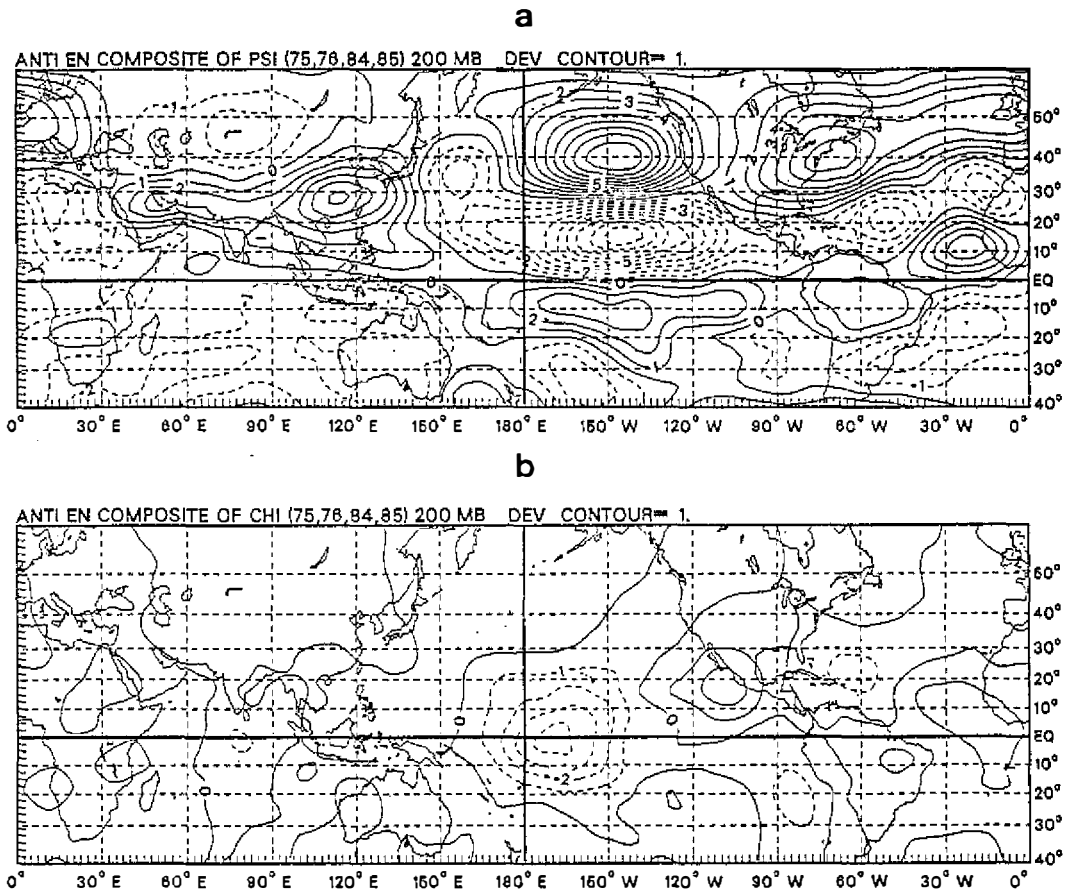
a

b

Fig. 4. As in *Fig.* 3 except for the four Anti-El Nino winters.

major divergent center in the equatorial central Pacific is surrounded by several convergent centers. The one immediately to the north (near 180°E, 28°N) delineates a "local Hadley cell." Two centers to the west, one in the MC area representing a negative MC anomaly and another near the northeast coast of Australia, provide termination points for the westward outflows of Walker-type circulations. To the east the divergent outflow connects to another convergent center southwest of Mexico to form another Walker-type circulation. This convergent center, although weak in magnitude, is situated to the immediate north of the time-mean χ center in the equatorial eastern Pacific (Fig. 1b), the one that is missing in NWP based time-mean fields as mentioned in Section 3.

In the Anti-El Nino composite the anomalous χ field (Fig. 4b) shows a major convergence center in the equatorial central Pacific, with an axi-symmetric distribution such that the reversed local Hadley and Walker type circulations, as well as convergent flow from other directions, all have about the same strength
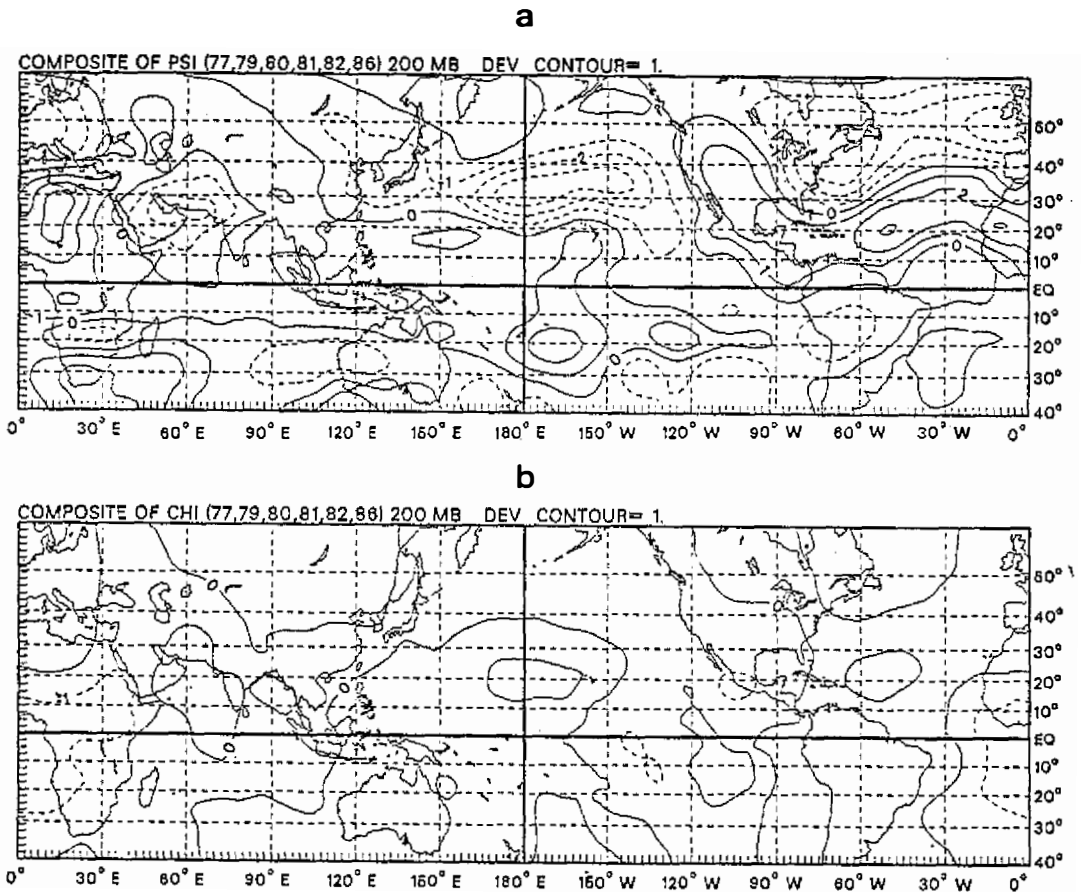
a

COMPOSITE OF PSI (77,79,80,81,82,86) 200 MB   DEV CONTOUR= 1.

b

COMPOSITE OF CHI (77,79,80,81,82,86) 200 MB   DEV CONTOUR= 1.

Fig. 5. As in *Fig.* 3 except for the six winters that do not belong to either El Nino or Anti-El Nino.

and extent. However, in the surrounding area only one divergent center clearly stands out. It is located southwest of Mexico in the same vicinity as the convergent center in the El Nino case. Thus this appears to be another important region for interannual variations in tropical divergent motions.

The second way of compositing is according to the variation of the divergence anomalies over the MC area. The seven winters where the MC χ anomalies are positive are also listed in Table 1. The results are shown in Fig. 6. In this composite the negative PNA teleconnection pattern also appears in the ψ field (Fig. 6a), although the intensity of the pattern is weaker than that of the Anti-El Nino composite (Fig. 4). Other ψ distribution within the broad Asia-Pacific region is also basically similar to the Anti-El Nino composite. An important difference is that in the MC composite the Australian ψ cell is stronger while the ψ cell in the south central Pacific is weaker. This leads to greater antisymmetry

about the equator in the MC longitudes and less in the central Pacific, consistent with linear equatorial wave theory.
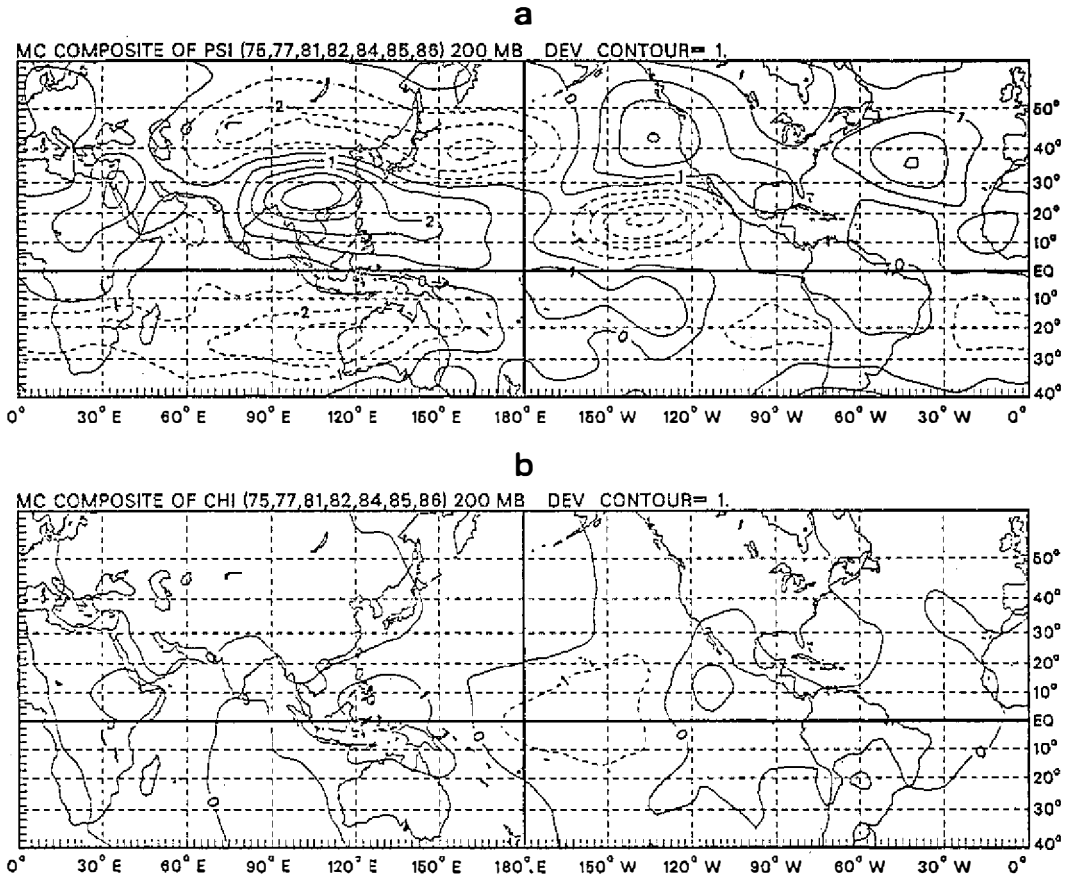
a

b

Fig. 6. As in *Fig.* 3 except for the seven winters that the χ anomalies in the maritime continent are positive.

The χ field (Fig. 6b) shows three tropical divergence features. The composite criterion naturally leads to an anomalous divergence center over the MC area. This center is not apparent in the Anti-El Nino case (Fig. 4b). Otherwise the major centers are similar to, but less prominent than, those in Fig. 4b, with a convergence center in the equatorial central Pacific and a divergence center off Mexico. The divergence center over the MC area is also of modest intensity, which is indicative of the varied distribution of χ anomalies in the seven winters. The removal of three (1974-75, 1983-84, 1984-85) of the seven winters that also belong to the Anti-El Nino category does not change significantly the gross features of the ψ and χ composite patterns.

The MC composite turns out to be somewhat different from that done by Lau and Boyle (1987), who composited a 9-year subset of the same data according to the OLR data. Instead of computing anomalies from the the long term mean, they subtracted the ψ and χ of the three maximum OLR (weak convection over MC) winters from those of the three minimum OLR (strong convection over MC) winters. Of the three winters they chose for minimum OLR activity over the MC vicinity, two (1980-81 and 1981-82) are included in the seven winters chosen in the present study. The resultant difference field in ψ, presumably representing the effect of strong convection in the MC area, is similar to Fig. 6a in the overall pattern. The exception is in the eastern North Pacific where Lau and Boyle's (1987) result shows a slanted negative PNA pattern such that the north Pacific positive ψ center at 135°W in Fig. 6a is situated over the western U.S. around 105°W in their Fig. 13c. This slanted negative PNA pattern occurs despite the fact that two of their three weak MC convection winters were El Nino (1977-78 and 1982-83) years.

In addition to the negative PNA pattern, both the Anti-El Nino and the MC ψ composites show a pattern of highs and lows suggestive of a wave train emanating from the MC area northeast- ward across the northwestern Pacific, and joining with the positive cell in the northeastern Pacific. In fact, a similar pattern with an opposite sign can also be identified in the El Nino composite, although the track is less well-defined, with the intermediate cell in the northwestern Pacific shifted to the southeast. The generally opposite patterns between the El Nino and the MC ψ composites are consistent with the generally out- of-phase relationship between the CP. and the MC χ anomalies. However, this makes it difficult to identify the respective roles played by the two possible tropical sources on the two teleconnection (PNA and MC wave train) patterns.

5. CORRELATIONS BETWEEN STREAMFUNCTION FIELD AND LOCAL DIVERGENCE IN THE EQUATORIAL BELT

In addition to compositing according to preconceived categorizations, the data are subjected to a single-point correlation analysis. Here the velocity potential at different longitudes of the equatorial belt is used as the "base point" to correlate with the velocity potential and streamfunction at all other grid points. Each base point is an area-average over a section between 10°S-10°N and 30° longitude in width. Because there are only 14 winter seasons in the data set, it may not be very meaningful to discuss the significance level of these correlations. Rather, the single point correlation may be regarded as a fast and convenient way to composite the ψ and χ anomalies according to χ variations at different equatorial longitudes. The large-scale distribution of positive and negative correlation patterns can be viewed as the composite

patterns of the 14 seasons, and the magnitude of the center values can be viewed as the relative magnitude of the composite features.

Figs. 7a-d show the correlations with global χ using the equatorial χ in the 120°W-90°W, 150°W-120°W, 180°W-150°W (CP) and 150°E-180°E sections, respectively, as the base point. A well defined out-of-phase correlation between the central Pacific divergence and the maritime continent divergence is indicated by negative correlation coefficients > 0.7 in the latter area in Figs. 7b-c. The negative correlation coefficients area spreads northeastward north of the equator and southeastward south of the equator, giving a symmetric "slanted wing" appearance in the western Pacific. In both hemispheres this structure can be traced to the midlatitudes, beyond 40°. It is interesting that while the southern wing resembles the SPCZ pattern, no similarly prominent climatological convective feature has been observed for its northern counterpart. This symmetric "slanted wing" distribution in the interannual variations of the tropical western Pacific divergence was not observed in previous studies using OLR data (e.g., Lau and Boyle, 1987). When the base point is shifted to the eastern extreme of the eastern Pacific (Fig. 7a) or west of the dateline (Fig. 7d), no large area of strong correlations are found outside of the base point.

Figs. 8a and 8b show the correlations with ψ using the equatorial velocity potential in the 150°W-120°W and 180°W-150°W (CP) sections, respectively, as the base point. Consistent with the El Nino and Anti-El Nino composites, the CP (Fig. 8b) correlation clearly exhibits the classical PNA pattern over the North Pacific, with the positive correlation maximum > 0.8 near 10°N and 150°W, and the negative correlation maximum > 0.9 just off the northwest coast of the United States. Further downstream, a negative center over the North Atlantic with a smaller correlation (> 0.6) is also indicated. As the base point is shifted 30° to the east (Fig. 8a), all these features basically remain. The subtropical positive correlation center is shifted only about 10° eastward to a position that is due north of the base point, with a slightly weaker maximum of > 0.7. The northwestern U.S. negative correlation center remains at about the same location but is reduced to > 0.6, and a stronger negative center of > 0.7 is found to the southeast near 30°N, 105°W.

In the southern tropics, both figures show a maximum negative correlation zone south of the equator in the general area of the base-point. As mentioned before, this approximate anti-symmetry about the equator is consistent with barotropic vorticity dynamics for divergent forcing at the equator. Fig. 8a exhibits this anti-symmetry better than Fig. 8b, where the anti-symmetry is somewhat distorted in a northeast-southwest orientation. On the other hand, in the longitudes of the maritime continent, a well formed anti-symmetric pattern of the opposite sign is found in Fig. 8b. This may be a manifestation of the out-of-phase correlation between the CP and the MC divergence as is evident
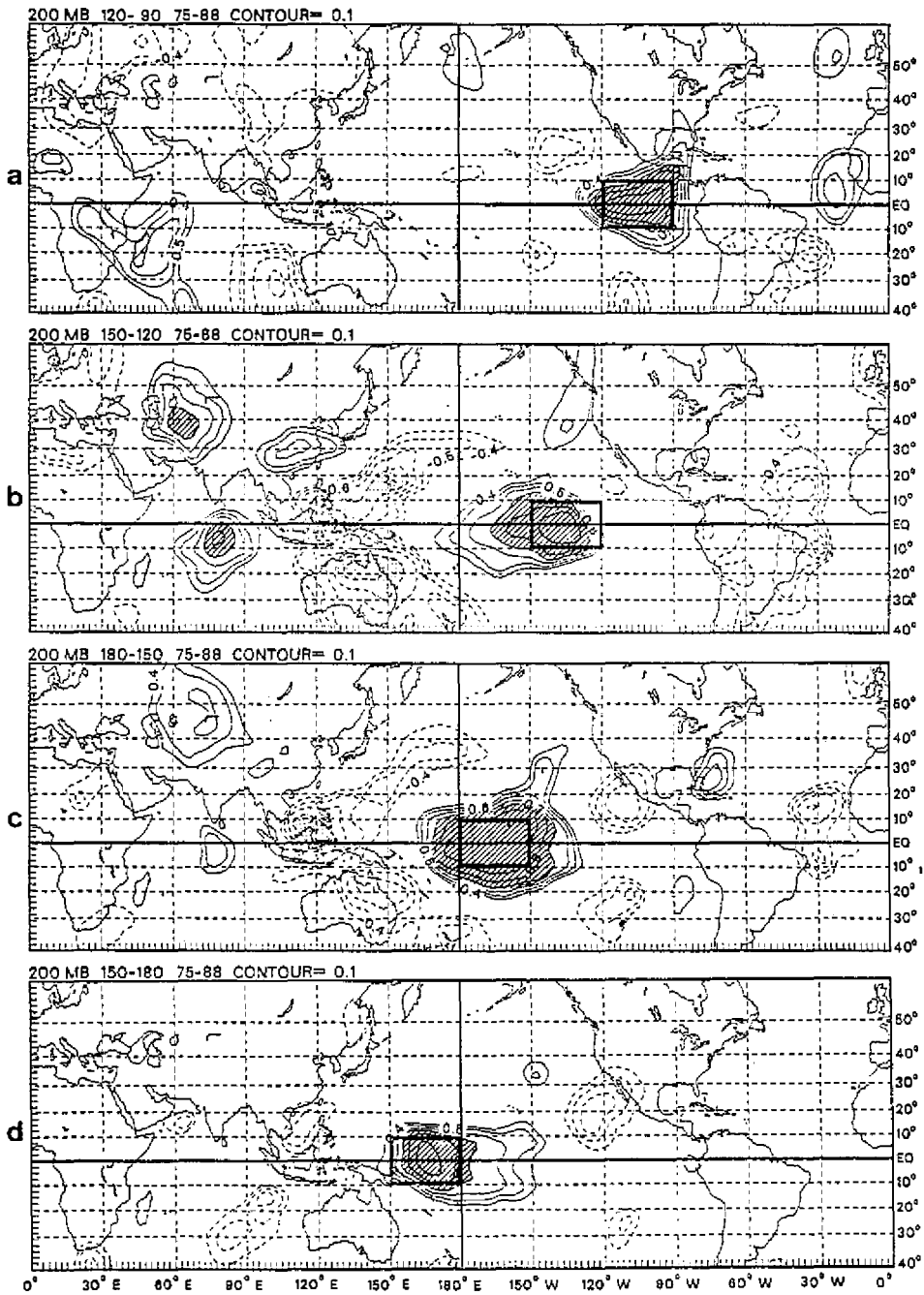
Fig. 7. Correlations with global χ using the area-averaged equatorial χ in the (a) 120°W-90°W, (b) 150°W-120°W, (c) 180°W-150°W (CP) and (d) 150°E-180°E sections, respectively, as the base point (marked by heavy rectangular at the equator). Shaded areas denote magnitude of correlation coefficients > 0.7.
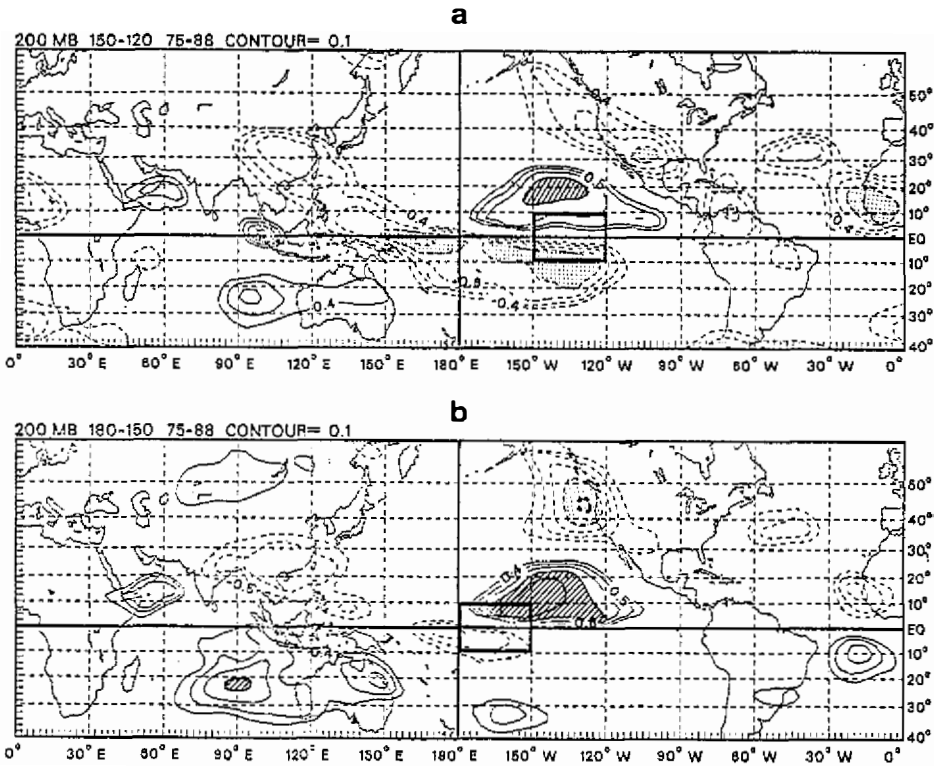
a

200 MB 150-120 75-88 CONTOUR= 0.1

b

200 MB 180-150 75-88 CONTOUR= 0.1

Fig. 8. Correlations with global ψ using the area-averaged equatorial χ in the (a) 150°W-120°W and (b) 180°W-150°W (CP) sections, respectively, as the base point (marked by heavy rectangular at the equator). Shaded areas denote magnitude of correlation coefficients > 0.7.
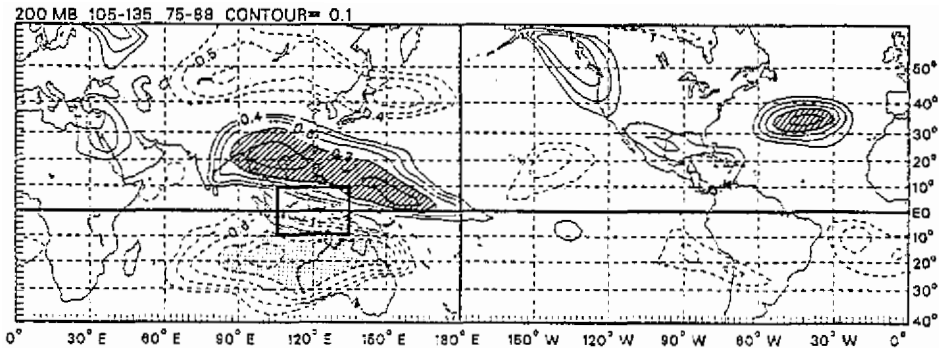
200 MB 105-135 75-88 CONTOUR= 0.1

Fig. 9. As in *Fig.* 8 except for area-averaged equatorial χ in the 105°E-135°E (MC) section as the base point.

in the χ-χ correlation (Fig 7).

Fig. 9 shows the correlations with the equatorial velocity potential in the

105°E-135°E (MC) section as the base point. Here the anti-symmetric pattern about the equator shows up even more prominently. The center values are > 0.8 on both sides of the equator, larger than those for the anti-symmetric pattern shown in Fig. 8b. The northern tropical positive correlation zone has two maximum, with the western one at 20°N, 105°E appearing to be a source for a possible wave train from the northwestern Pacific to an area off western Canada. Further downstream of this wave train, a positive correlation maximum > 0.8 is found in the North Atlantic, at the same location of a negative center found in the CP base point correlation. The negative PNA pattern over the North Pacific can also be identified, but the correlation is considerably weaker.

It is possible to trace the signal of a wave train pattern from southern China to the northwestern U.S in Figs. 8a and 8b as well (particularly Fig. 8b), but with opposite signs to those in Fig. 9. This may again be expected from the out-of-phase relationship between the two major centers of tropical divergence anomalies. However, the MC base point correlation gives a much stronger wave train definition. This suggests that this East Asia-North Pacific wave pattern is more directly related to the divergence anomalies over the MC area. Similarly, a comparison of the PNA correlation pattern between Figs. 8 and 9 suggests that the PNA pattern is more directly related to the CP divergence anomalies. Both effects have a teleconnection influence over the same area off the northwestern coast of North America, with the two influences appearing to take quite different routes.

Figs. 8a and 8b suggest a modest sensitivity of the ψ "response" to the longitudinal position of the equatorial χ "forcing" in the central Pacific. To examine this sensitivity further, a series of six equatorial χ-global ψ correlation maps, with the χ base point moving from 120°W-90°W westward to 90°E-120°E at 30° intervals, is displayed in Fig. 10. (The MC base point map shown in Fig. 9 is an intermediate map between Figs. 10e and 10f.) Fig. 10a shows that there is no PNA pattern when the χ-base point is in the eastern end of the eastern Pacific between 120°W-90°W. Between 120°W and the dateline, the PNA pattern is clearly identifiable in the eastern Pacific (Fig. 10b and 10c, same as Fig 8). The pattern becomes very weak as the base point is shifted to the west of the dateline (Fig. 10d), and the negative PNA pattern appears in the eastern Pacific when the base point is between 150°E-120°E (Fig. 10e). This is also when a strong positive-correlation ψ "response" reappears immediately north of the equatorial χ-base point region. In this case it is over the eastern part of the MC. Further north there is an indication of a negative correlation cell response over Japan.

If the base point is now shifted 15° to the west, we get Fig. 9, which shows the East Asia-North Pacific wave train pattern. As the base point is shifted further west to cover the western part of the MC (Fig. 10f), the northern
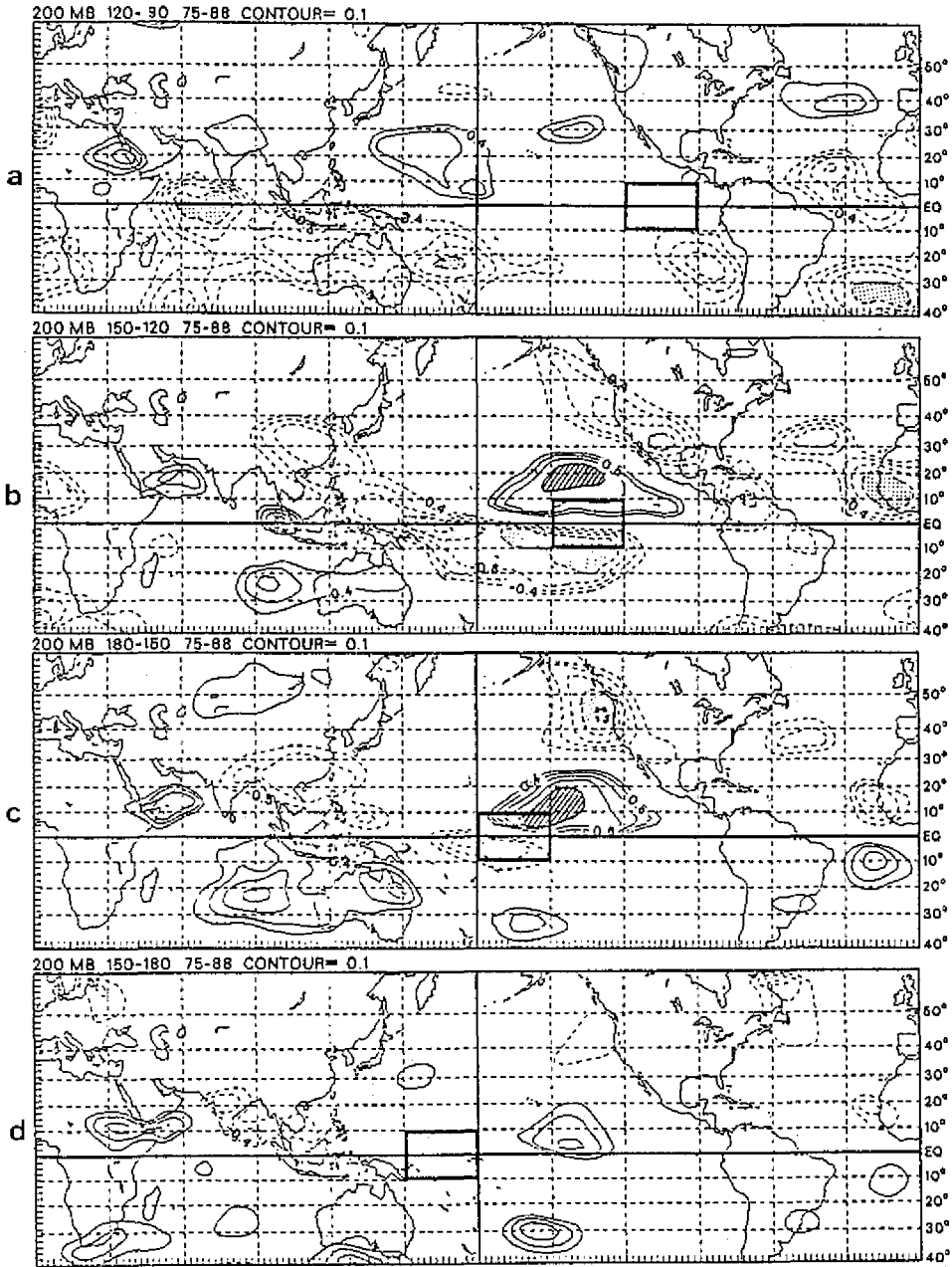
Fig. 10. As in *Fig.* 8 except for a series of six equatorial χ-global ψ correlation maps, with the χ base point section moving from 120^oW-90^oW westward to 90^oE-120^oE. See text for details.

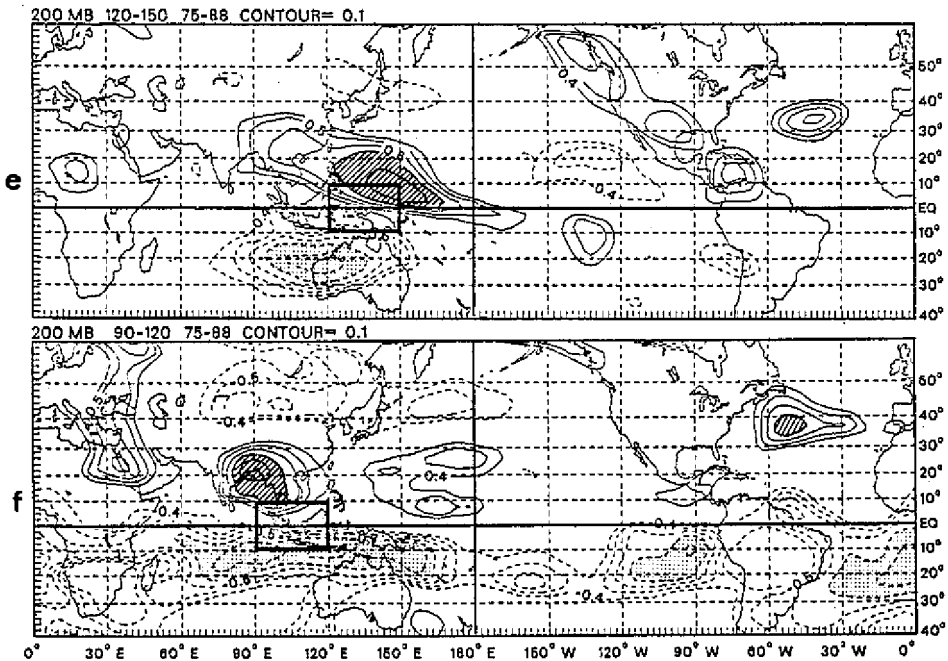equatorial positive-correlation cell is shifted westward as well. This cell may still

Fig. 10. (Continued)

be identified as an upstream part of a wave train that is traceable northeastward. A positive cell downstream over the northwestern North America, but a negative PNA pattern is not apparent in the eastern Pacific.

Based on Fig. 10, it appears that considerable sensitivity to the longitude of equatorial divergent anomalies exists in the midlatitude North Pacific "response." The PNA teleconnection pattern is relatively insensitive only when the divergence anomaly is located within the longitudinal band, between 150°E-120°W. (Strictly speaking the band is from 180°W to 120°W. Between 150°E-180°E the correlated PNA pattern is very weak. However, this may be due to the smaller variability of the divergence there.) The PNA pattern is not identifiable when the anomaly is located east of this band. When the anomaly is moved westward of this band, the primary pattern changes first to a negative PNA and then to a East Asia-North Pacific wave train.

The χ-χ and χ-ψ correlations have also been done using individual months. The monthly anomalies are computed from the long-term means of the respective months (e.g., December anomaly is the departure from the average of 14 Decembers), so that each time series consists of 42 independent points. The resultant correlation patterns (not shown) are very similar to the correlations using the 14-point winter data, with the correlation values at positive and neg-

atives centers decreased typically by 0.1. This means that, in general, the significance level for all areas enclosed by a 0.7 isopleth in Figs. 7-10 (0.6 in the 42-point correlations) is > 99.5 %.

6. SUMMARY AND CONCLUDING REMARKS

a

85-86 ANOMALY OF PSI 200 MB   DEV CONTOUR= 2.

b

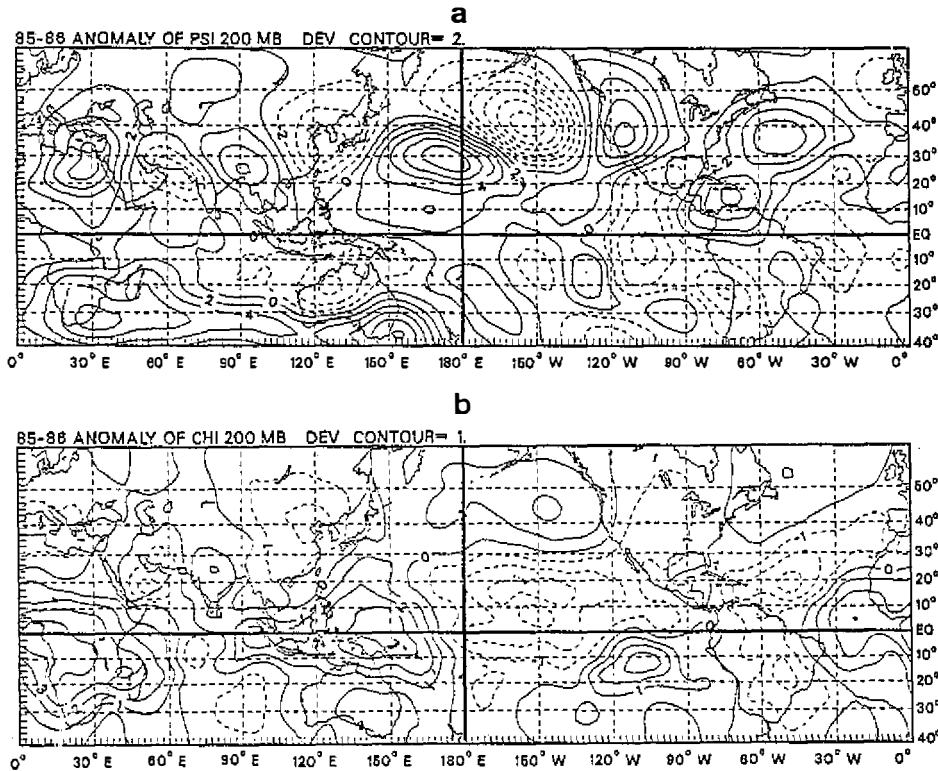85-86 ANOMALY OF CHI 200 MB   DEV CONTOUR= 1.

Fig. 11. The (a) streamfunction and (b) velocity potential anomalies for the winter of 1985-1986.

Using 14 winters of divergence data analyzed directly from observations, the interannual variations of the tropical Pacific divergence at 200 *mb* are studied with composite and single-point correlation methods. The two prominent centers of the divergence variations in the equatorial Pacific are located in the central Pacific, which has been related to El Nino events, and the maritime continent area. Neither of these two centers are located in the center of the long-term mean divergence. Single point correlations show that the interannual variations of the maritime continent divergence, which has been known to be out-of-phase with the central Pacific divergence, have a "slanted wing" structure that is symmetric about the equator and extends into midlatitudes in both
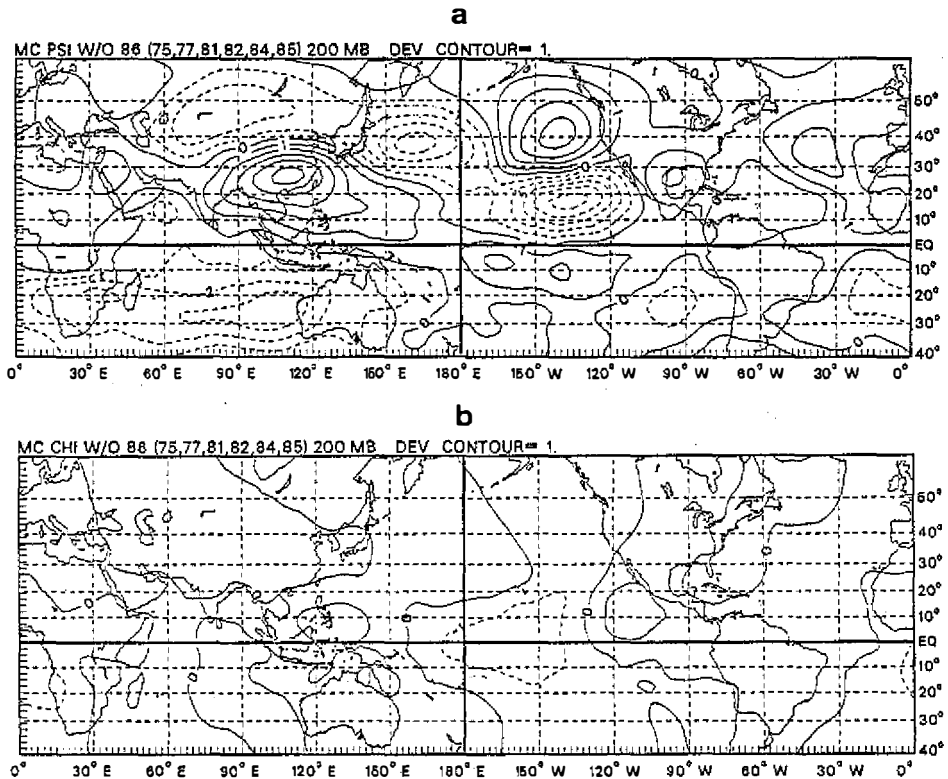
a

MC PSI W/O 86 (75,77,81,82,84,85) 200 MB   DEV CONTOUR= 1.

b

MC CHI W/O 86 (75,77,81,82,84,85) 200 MB   DEV CONTOUR= 1.

Fig. 12. As in *Fig.* 6 except for only six MC cases, with the 1985-1986 winter excluded.

hemispheres. The south wing resembles the SPCZ while the north wing is not obvious in satellite cloud data. A third major center of interannual variations is identified southwest of Mexico. This center is also out-of-phase with the one in the central Pacific.

The present results provide support for the importance of equatorial divergence forcing of positive and negative PNA patterns from the equatorial central Pacific, and for a northeastward wave train across the North Pacific from the maritime continent. The two teleconnection patterns give opposite influences to the streamfunction over the northeastern Pacific near the northwestern coast of North America. However, the insensitivity of teleconnection patterns with respect to the longitude of tropical SST anomalies, as reported by some previous GCM studies, can be observed only within a limited region. This result is derived from examining the single-point correlation patterns between equatorial velocity potential at varios base points and global streamfunction. In the northern Pacific, the PNA correlation pattern is basically robust only when the base point velocity potential is within the 180°W-120°W region. The pattern changes rapidly when the base point is moved outside of this region.

Close inspection of individual seasons' anomaly charts indicates that the teleconnection patterns are quite complex and can vary greatly. One example is the winter of 1985-1986, whose streamfunction anomaly has the most prominent East Asia-North Pacific wave train pattern of all the years. This pattern appears to emanate from a western Pacific χ anomaly center (Fig. 11). Within this season the wave train is strikingly noticeable from December 1985 to January 1986 (Hoskins and Sardeshmukh, 1987). The 1985-86 winter is also one of the seven winters used in the maritime continent composite (Fig. 6). Thus, it may be expected that this season contributes strongly to the appearance of the wave train in the maritime continent composite. However, in the subtropics the wave train axis in the 1985-86 ψ anomaly is approximately 50° to the east of the composite axis, so that the inclusion of this winter actually makes the composite wave train less distinct. (The equatorial χ center in 1985-86 is also shifted about 25° to the east.) If this season is removed, the composite of the other six MC cases gives a wave train (Fig. 12) that is more distinct than Fig. 6 due to significantly larger amplitudes of the downstream cells in the northwestern and northeastern Pacific. Similarly, the MC χ- ψ correlation diagram defines a more focused wave train pattern emanating from the χ base-point sector when the 1985- 86 data is removed (not shown). Thus the composite and correlation approaches may sometimes mask important features. It is therefore important to supplement the composite study by diagnostic or modeling studies of individual season's anomalies.

REFERENCES

Arkin, P. A., V. E. Kousky, J. E. Janowiak, and E. A. O'Lenic, 1986: Atlas of the tropical and subtropical circulation derived from National Meteorological Center Operational Analyses. NOAA Atlas No. 7, 8pp [Available from Climate Analysis Center, NOAA/NMC, Washington, D. C. 20233]

Blackmon, M. L., G. W. Branstator, G. T. Bates and J. E. Geisler, 1987: An analysis of equatorial Pacific sea surface temperature anomaly experiments in general circulation models with and without mountains. *J. Atmos. Sci.*, **44**, 1828-1844.

Boyle, J. S. and C.-P. Chang, 1984: Monthly and seasonal winter climatology over the global tropics and subtropics for the decade 1973 to 1983. Vol.

I. 200 *mb* winds. Naval Postgraduate School Tech. Rept. 63-84-006, 172pp. [Available from Dept of Meteorology, Naval Postgraduate School, Monterey, CA 93943.]

Branstator, G. W., 1985: Analysis of general circulation model sea-surface temperature anomaly simulation using a linear model. Part I: Forced solution. *J. Atmos. Sci.*, **42**, 2225-2241.

Chang, C.-P. and H. Lim, 1983: Dynamics of teleconnections and walker circulations forced by equatorial heating. *J. Atmos. Sci.*, **40**, 1897-1915.

Chang, C.-P. and K. G. Lum, 1985: Tropical-midlatitude interactions over Asia and the western Pacific Ocean during the 1983-84 northern winter. *Mon. Wea. Rev.*, **113**, 1345-1358.

Geisler, J. E., M. L. Blackmon, G. T. Bates and S. Munoz, 1985: Sensitivity of January climate response to the magnitude and position of equatorial Pacific sea surface temperature anomalies. *J. Atmos. Sci.*, **42**, 1037-1049.

Gill, A. E., 1980: Some simple solutions for heat-induced tropical circulation. *Quart. J. Roy. Meteor. Soc.*, **106**, 447- 462.

Hendon, H. H., 1988: A qualitative assessment of the Australian Tropical Region Analyses. *Mon. Wea. Rev.*, **116**, 5-17.

Horel J. D., and J. M. Wallace, 1981: Planetary scale atmospheric phenomena associated with the southern oscillation. *Mon. Wea. Rev.*, **109**, 813-829.

Hoskins, B. J. and P. D. Sardeshmukh, 1987: A diagnostic study of the dynamics of the northern hemisphere winter of 1985-86. *Quart. J. Roy. Meteor. Soc.*, **113**, 759-778.

Kashahara, A. and P. L. Silva Dias, 1986: Response of planetary waves to stationary tropical heating in a global atmosphere with meridional and vertical shear. *J. Atmos. Sci.*, **43**, 1893- 1911.

Kousky, V. E. and A. Leetmaa, 1989: The 1986-87 Pacific warm episode: Evolution of oceanic and atmospheric anomaly fields. *J. Climate*, **2**, 254-267

Krishnamurti, T. N., M. Kanamitsu, W. J. Koss and J. D. Lee, 1973: Tropical east-west circulation during the northern winter. *J. Atmos. Sci.*, **30**, 780-787.

Lambert, S.J., 1989: A comparison of divergent winds from the National Meteorological Center and the European Centre for Medium Range Weather Forecasts global analyses for 1980-1986. *Mon. Wea. Rev.*, **117**, 995-1005.

Lau, K. M., and J. S. Boyle, 1987: Tropical and extratropical forcing of the large-scale circulation: A diagnostic study. *Mon. Wea. Rev.*, **115**, 400-428.

Lau, K. M., and C.-P. Chang, 1987: Planetary scale aspects of the winter monsoon and atmospheric teleconnections. *Monsoon Meteorology*, C.-P. Chang and T. N. Krishnamurti, eds., Oxford University Press, 161-202.

Lewis, J. M. and T. H. Grayson, 1972: The adjustment of surface wind and

pressure by Sasaki's variational matching technique. *J. Appl. Meteor.*, **11**, 586-597.

Lim, H. and C.-P. Chang, 1986: Generation of internal- and external-mode motions from internal heating: effects of vertical shear and damping. *J. Atmos. Sci.*, **41**, 948-957.

Livezey, R. T. and K. C. Mo, 1987: Tropical-Extratropical Teleconnections during the northern hemisphere winter. Part II: Relationships between monthly mean northern hemisphere circulation patterns and proxies for tropical convection. *Mon. Wea. Rev.*, **115**, 3115-3132.

Murakami, T. and Unninayar, 1977: Atmospheric circulation during December 1970 through February 1971. *Mon. Wea. Rev.*, **105**, 1024-1038.

Palmer, T. N. and J. A. Owen, 1986: A possible relationship between some "severe" winters in North America and enhanced convective activity over the tropical West Pacific. *Mon. Wea. Rev.*, **114**, 648-651.

Pitcher, E.J., M.L. Blackmon, G.T. Bates and S. Munoz, 1988: The effect of North Pacific sea surface temperature anomalies on the january climate of a general circulation model. *J. Atmos. Sci.*, **45**, 173-188.

Sardeshmukh, P. and B. J. Hoskins, 1988: The generation of global rotational flow by a steady idealized tropical divergence. *J. Atmos. Sci.*, **45**, 1228-1251.

Shukla, J. and K. R. Saha, 1974: Computation of non-divergent streamfunction and irrotational velocity potential from the observed winds. *Mon. Wea. Rev.*, **102**, 419-425.

Simmons, A. J., J. M. Wallace and G. W. Branstator, 1983: Barotropic propagation and instability, and atmospheric teleconnection patterns. *J. Atmos. Sci.*, **40**, 1363-1392.

Trenberth, K. E. and J. G. Olson, 1988: An evaluation and intercomparison of global analyses from the National Meteorological Center and the European Centre for Medium Range Weather Forecasts. *Bull Amer. Met. Soc.*, **69**, 1047-1057.

Unden, P. 1989: Tropical Data Assimilation and Analysis of Divergence. *Mon. Wea. Rev.*, **117**, 2495-2517.

Wallace, J. M. and Q. Jiang, 1987: On the observed structure of the interannual variability of the atmosphere/ocean climate system. *Atmos. and Oceanic Variability*, H. Cattle, ed., Roy. Met. Soc., Bracknell, Berks, 17-43.

Webster, P. and H. R. Chang, 1988: Tropical accumulation and emanation: Wave propagation through a zonally varying basic state. *J. Atmos. Sci.*, **45**, 803-829.

Weickman, K. M. and S. J. S. Khalsa, 1990: The shift of convection from the Indian Ocean to the Western Pacific Ocean during a 30-60 day oscillation. *Mon. Wea. Rev.*, **118**, 964-978.

冬季熱帶對流層高空輻散場之年際變化與太平洋區之遙相關

張智北 M. S. Peng J. S. Boyle

美國海軍研究學院氣象系

摘　　要

　　本文採用美國海軍十五年間(1974～1988)熱帶分析資料以研究太平洋區冬季 200毫巴氣流之年際變化。與一般作業資料不同，此資料之輻散場不受數值模式預報之影響，同時此資料亦與平均時間長波輻射資料較相近。資料分析結果顯示赤道區有兩主要之大尺度輻散距平中心，其一位於太平洋之中部另一位於西太平洋印尼、菠蘿洲一帶，而此二輻散距平則呈反相之變化。第三個主要之輻散距平中心在墨西哥西岸之西南方，此距平中心亦和太平洋中部之距平中心亦呈異相之變化。

　　由複合或單點相關計算結果皆顯示遙應型態和赤道區輻散距平間有重要之相互關係，尤其是太平洋中部之輻散是促成 PNA型態之重要外力，而印尼、菠蘿洲一帶之輻散則是促成北太平洋東北向波群型態之主要外力。這兩種遙相關型態在東北太平洋之流線函數距平互成異號。

　　我們進一步將輻散基點沿著赤道帶移動觀看相關係數值改變之情形，由此計算之結果顯示有些由環流模式模擬結果所得"遙相關型態隨熱帶外力位置改變並不敏感"之說法只在相當有限之範圍內才正確，在太平洋熱帶區如赤道之輻散基點在150°E和120°W間移動時PMA 相關型態只做小輻度之改變，但將基點移出比範圍時，相關型態會有非常明顯的改變。